CHAPTER 3

Observations and Data Reduction

In this study, the CCD images of the open clusters NGC 2126 and NGC 1528 were collected with the main purpose to study variable stars in the open clusters. Images of NGC 2126 were observed in different seasons from beginning of March 2004 until March 2015 separated into three observation runs; the first period was between 24th and 31st March 2004 using the 1-m robotic telescope at the Mount Lemmon Optical Astronomy Observatory (LOAO) in Arizona, then between 12th January and 9th February 2013 using the 2.4-m Thai National Telescope (TNT). The last period, between 16th and 21st March 2015 using the 0.5-m Corrected Dall-Kirkham PlaneWave CDK24 remote-controlled telescope located at the Thai National Observatory (TNO). Original observations in 2004 were performed for searching the new variable stars and to study the pulsations of the oEA star which is an Algol type eclipsing binary with a pulsating component (Mkrtichian et al., 2007) in the cluster.

Images of NGC 1528 were observed in the year 2003 and 2007 separated into two observation runs; the first period was between 15th October and 8th December 2003, then between 21st September 2006 and 27th March 2007 using a 40-cm f4.9 Newtonian telescope equipped with a ST10XME camera at the Beersel Hills Observatory (BHO), Beersel, Belgium. Field of view is 17.2×25.5 arcmin^2. A total of 1482 images was obtained in the V band. The differential photometry was applied to the data.

3.1 Telescopes and Instruments

3.1.1 The 1-m Telescope at Mount Lemmon Optical Astronomy Observatory

A 1-m robotic telescope at Mount Lemmon, Arizona, was installed by Korea Astronomy and Space Science Institute (KASI) in collaboration with a company, Astronomical Consultants and Equipment, Inc (ACE) in the early 90's. The telescope system is designed

for remote observations and it also can be used in interactive robotic mode. Both optical and mechanical parts of the telescope are newly designed. The telescope mount is an equatorial fork with tracking speeds of about $15'' \ s^{-1}$. A tracking accuracy is about $\pm 5'' \ hr^{-1}$. In order to correct for mechanical errors, the integral pointing model is included in the mount system. The optical system is an f/7.5 Ritchey-Chretien which can collect 80% of the incident light within $0.5''$. An all sky camera and weather station are installed at the observatory to obtain daily environmental information (Han et al., 2005).

In 1998, KASI retrofitted the telescope system in collaborate with the company ACE (Astronomical Consultants & Equipment). In that time, the existing 1-m telescope was dismantled to install again. The telescope optics and other items were installed for a new telescope. The company ACE manufactured the new control system. The telescope optics were re-configured for a wider FOV after optical performance tests were completed in 1999. The design concept of the system was introduced by Han et al. (2000), The robotic system was presented by Mack et al. (2001a), and the pointing software was discussed by Mack et al. (2001b). A newly polished mirror was constructed at the site in late 2002. An experimental follow-up observation project named the ROTSE survey was proceeded for 1 year after the system was completed. Since late 2003, the interactive remote control of the telescope is being regularly used for astronomical research from Korea.

Detectors and Filter Wheels

There are two wheels in the filter box, which 10 filters can be placed for each wheel. 18 filters can be installed in the same time because the wheels are stacked. The double wheel system is very useful because multi-color photometric filters are loaded in the lower wheel and neutral-density filters can be placed in the upper wheel. For a lower limit of position repeatability of 10 μm, the wheels are equipped with a precision detent lock and absolute encoders. The importance of detent lock is to control the motor power to be automatically turned off when the wheel is not moving. Presently, Cousins R_cI_c filters and five filters of Johnson UBV are available. The telescope has been installed with a thermoelectrically cooled KODAK 4300E detector (2084×2084 array), which is a large-format CCD from Finger Lakes Instruments. This CCD provides an image with the filed

Figure 3.1: The Mount Lemmon Optical Astronomy Observatory, Arizona (LOAO) is located on Mount Lemmon in the Santa Catalina Mountains approximately 28 kilometers northeast of Tucson, Arizona. (Credit image: http://skycenter.arizona.edu)

Figure 3.2: The 1-m Robotic Telescope at Mount Lemmon Optical Astronomy Observatory (LOAO). (Credit image: http://skycenter.arizona.edu)

Table 3.1: The parameters of optical system for the KASI 1-m telescope (Han et al., 2005)

Description	Specification
Primary mirror	
Diameter (physical)	1046 mm
Diameter (optical)	1000 mm
Diameter central perforation	141 mm
Radius of curvature	5509 mm
Focal ratio	2.633
Conic constant	-1.1092
Secondary mirror	
Diameter (physical)	332.4 mm
Diameter (optical)	330.4 mm
Radius of curvature	-2607 mm
Conic constant	-5.6389
System characteristics	
Effective focal length	7845 mm
Effective focal ratio	f/7.5
Field of view (diameter)	$28'$
Plate scale	$26.25''$ mm^{-1}

of view size of $22.2' \times 22.2'$. The image scale per pixel is $0.64''$, and it is very useful for aperture photometry.

3.1.2 The 2.4-m Thai National Telescope at Thai National Observatory

The Thai National Observatory (TNO) houses the 2.4-m Thai National Telescope (TNT), located on Doi Inthanon, the highest mountain in Thailand. The 2.4-m telescope is a reflecting telescope with an alt-azimuth drive system and a Ritchey-Chretien optical system. The system is synchronized with automatic control of the dome. The telescope is built at EOST in Tucson, Arizona, USA. The primary mirror of 2.4-m telescope has been fabricated and fine polished in Russia by LZOS facility. In 2012, the TNT was installed by the National Astronomical Research Institute of Thailand (NARIT) and stared first observation in the beginning of the year 2013. At 2,457 m high from sea level, observing conditions including photometric conditions and seeing are much better than that compare with other regions in Thailand. The observation season at this site starts from November until April, and remaining months are not suitable for observations because of rainy season and high humidity (Richichi et al., 2014).

Figure 3.3: The Thai National Observatory is the main observatory of the National Astronomical Research Institute of Thailand, located at km. 44 on Doi Inthanon), Chiang Mai, Thailand. (Credit image: http://www.narit.or.th)

Figure 3.4: The 2.4-m telescope at Thai National Observatory, Thailand. (Credit image: http://www.narit.or.th)

Table 3.2: The optical design parameters for the 2.4-m Thai National Telescope

Description	Specification
Primary Mirror Diameter	2.4 m ($\pm$ 10 mm)
Total Focal Length	24 m
System Focal Ratio	f/10
Plate Scale	8.6 arcsec/mm
Field of View	16 arc min
Total wavefront error	$<$140 nm rms at 0 Zenith angle

Detectors and Filter Wheels

A multi-instrument port was installed at the telescope. The permanently mounted detector is the ULTRASPEC instrument, which is the same type of detector has been used at the ESO New Technology Telescope in Chile (Dhillon et al., 2008; Ives et al., 2008). ULTRASPEC at the TNT was first used in the end of the year 2013 and Dhillon et al. (2014) introduced about this detector in detail. The Apogee U42 4 megapixel camera was also placed at the initial phase of the telescope, and it was removed until ARC camera becomes available. Currently, the detector is equipped with a set of Strömgren filters, *UBVRI*, *LRGB*.

Table 3.3: The scientific cameras available at Thai National Telescope

Designation	Format	Field of View	Main Goal
Apogee U42	2k$\times$2k	$4' \times 4'$	Test instruments, Early Science
ARC	4k$\times$4k	$8' \times 8'$	General purpose
ULTRASPEC	1k$\times$1k	$7.6' \times 7.6'$	Transients, Fast Readout Imaging
Point grey	1k$\times$1k	$42.4'' \times 42.4''$	Planet

3.1.3 The 0.5-m Telescope at Thai National Observatory

The other telescope at Thai National Observatory (TNO) is the 0.5-m Corrected Dall-Kirkham PlaneWave CDK24 remote-controlled telescope.

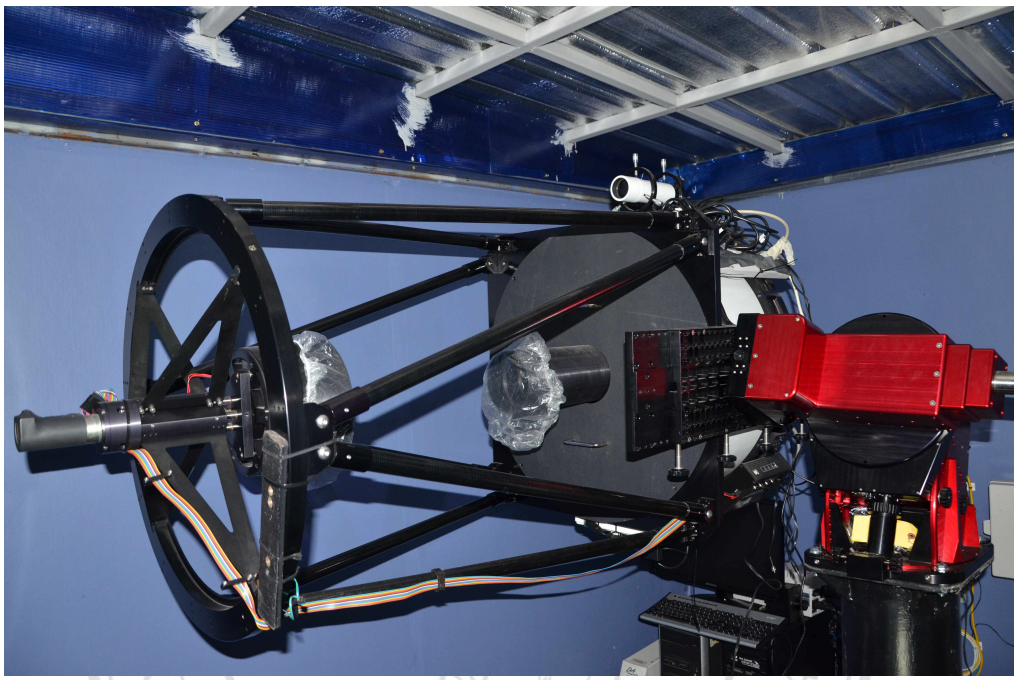

Figure 3.5: The 0.5-m telescope at Thai National Observatory, Thailand. (Credit image: http://www.narit.or.th)

Table 3.4: The model of the 0.5-m corrected Dall-Kirkham PlaneWave CDK24 remote-controlled telescope located at the Thai National Observatory (TNO).

Description	Specification
Aperture	50 cm (0.5 m)
Focal Length	3962 mm (155.98 inch)
Focal Ratio	f/6.5
Central Obstruction	47% of the Primary Mirror Diameter (11.38″)
Back Focus from Mounting Surface	14.1 inch (358 mm)
Optimal Field of View	70 mm (58 arcmin)

3.1.4 The 40-cm telescope at Beersel Hills Observatory (BHO), Belgium

A 40-cm f4.9 Newtonian reflector telescope located at Beersel Hills Observatory (BHO) which is located in Beersel, a village about 10 km southwest of Brussels. The Beersel Hills Observatory is a privately-owned astronomical observatory, which is primarily dedicated to the study of variable stars, including δ Scuti, eclipsing binaries, and

Table 3.5: The CCD model of Apogee Altra U9000 with L, R, G, B filter

Description	Specification
Array Size (pixels)	3056×3056
Pixel Size	12×12 microns
Imaging Area	36.7×36.7 mm (1345 mm^2)
Imaging Diagonal	51.9 mm
Linear Full Well (typical)	110K electrons
Dynamic Range	84dB
QE at 400nm	37%
Peak QE (550nm)	64%
Anti-blooming	>100X

visual double stars. The present observatory was founded in April 1998. Before that date, observations were carried out from another site but with the same instruments. The 40-cm f4.9 Newtonian reflector telescope is installed in the a 4.0-m rotating aluminium dome, which was manufactured by Roger Van Huffel. The mount system of the telescope is an equatorial computer controlled mount, which was manufactured by Astrotechniek. Recently this telescope was moved to another site. The dome now contains another telescope, which is an 180 mm APO refractor on an AP1200 mount.

Detectors and Filter Wheels

The 40-cm telescope is equipped with a ST10XME (SBIG) CCD camera. The camera is equipped with a filter wheel with $BVRI$ filters. The Model ST10XME is one of self-guiding CCD camera in the "ST" series from SBIG. The body of CCD camera is modified to accommodate with the larger detector. The ST10XME contains two CCDs, which is similar to other self-guiding cameras in the series. The guiding CCD is the TC-237H with 657×495 pixels. The imaging CCD is an enhanced KAF-3200ME imaging detector from Kodak with 3.2 million pixels. MaximDL-software is used to operate the camera.

3.2 The Characteristics of the Various Observations

The characteristics of the observational runs and of the various instruments including telescopes and CCD cameras (see Table 3.7) are the following:

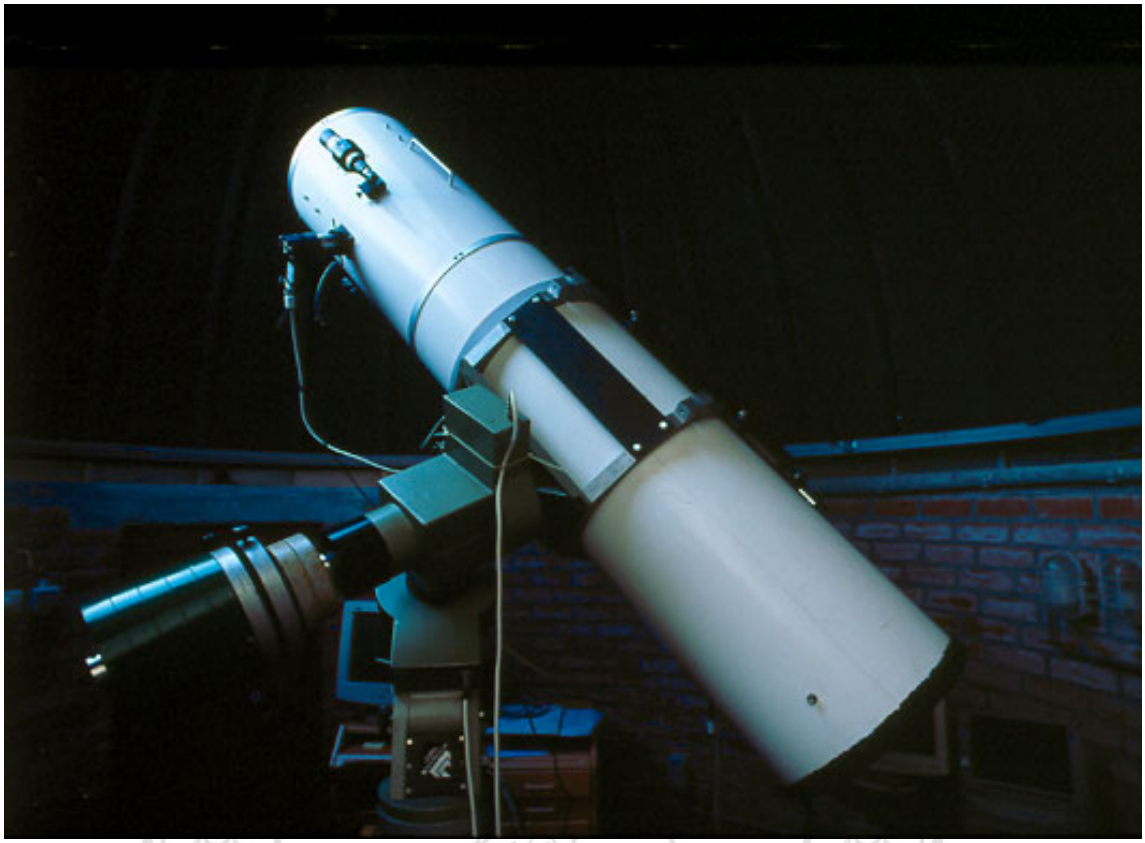

Figure 3.6: The 40-cm f4.9 Newtonian reflector telescope at Beersel Hills Observatory (Credit image: http://users.skynet.be).

Table 3.6: The CCD model of ST10XME (SBIG) camera

Description	Specification
CCD	Kodak KAF-3200ME+TI TC-237
Pixel Array	2184 x 1472 pixels
CCD Size	14.9 x 10 mm
Total Pixels	3.2 million
Pixel Size	6.8 x 6.8 microns square
Full Well Capacity	77,000 e^-
Dark Current	0.5 e^-/pixel/sec at 0 degrees C
Antiblooming	n/a

1) The first run of time-series observations of NGC 2126 was carried out during eight nights in January 2004 using the 1.0-m robotic telescope (Han et al., 2005) at Mount Lemmon Optical Astronomy Observatory (LOAO) using remote control from Korea via a network connection. The detector was 2k $\times$ 2k CCD camera. The field of view of a CCD image is about 22.2 $\times$ 22.2 arcmin^2 at the f/7.5 Cassegrain focus of the telescope. A total of 515 images

was obtained in the V-band filter, with an exposure time of about 100-300 s. The telescope was built as part of KASI long-term project aimed to survey variable stars in open clusters; extensive time-series CCD observations have been performed for intermediate-age open clusters. The main objectives is to search for short-period pulsating variables, such as δ Scuti and γ Dor type stars (Kang et al., 2007).

2) The second run of time-series observations was carried out during eight nights in January and February 2013 using the 2.4-m reflecting Thai national telescope (TNT) equipped with an alt-azimuth drive system and a Ritchey-Chrétien optical system at the Thai National Observatory (TNO). The detector was 2k $\times$ 2k Apogee U4200 CCD camera. The field of view of CCD covers about 5.5 $\times$ 5.5 arcmin^2. The filter system consists of B and V filters. A total of 456 images was obtained in the B and V bands, with an exposure time of about 200 s.

3) The third run of observations was performed for six nights in March 2015 using 0.5-m Corrected Dall-Kirkham PlaneWave CDK24 remote-controlled telescope located at the Thai National Observatory (TNO). The detector was an Apogee Altra U9000 3056 $\times$ 3056 pixel CCD camera. The field of view of CCD covers about 22.2 $\times$ 22.2 arcmin^2. For this observing run, a total of 411 images was obtained in the V filter, with an exposure time of about 100 s.

Tables 3.8 and 3.9 present the journal of the observations including the date, start time, length of observations, number of frames and the type of minimum for NGC 2126 and NGC 1528, respectively. Table 3.10 shows the coordinates from the UCAC4 catalogue of the reference and check stars for both clusters. Figures 3.7 and 3.9 present the fields of view covered by our observations.

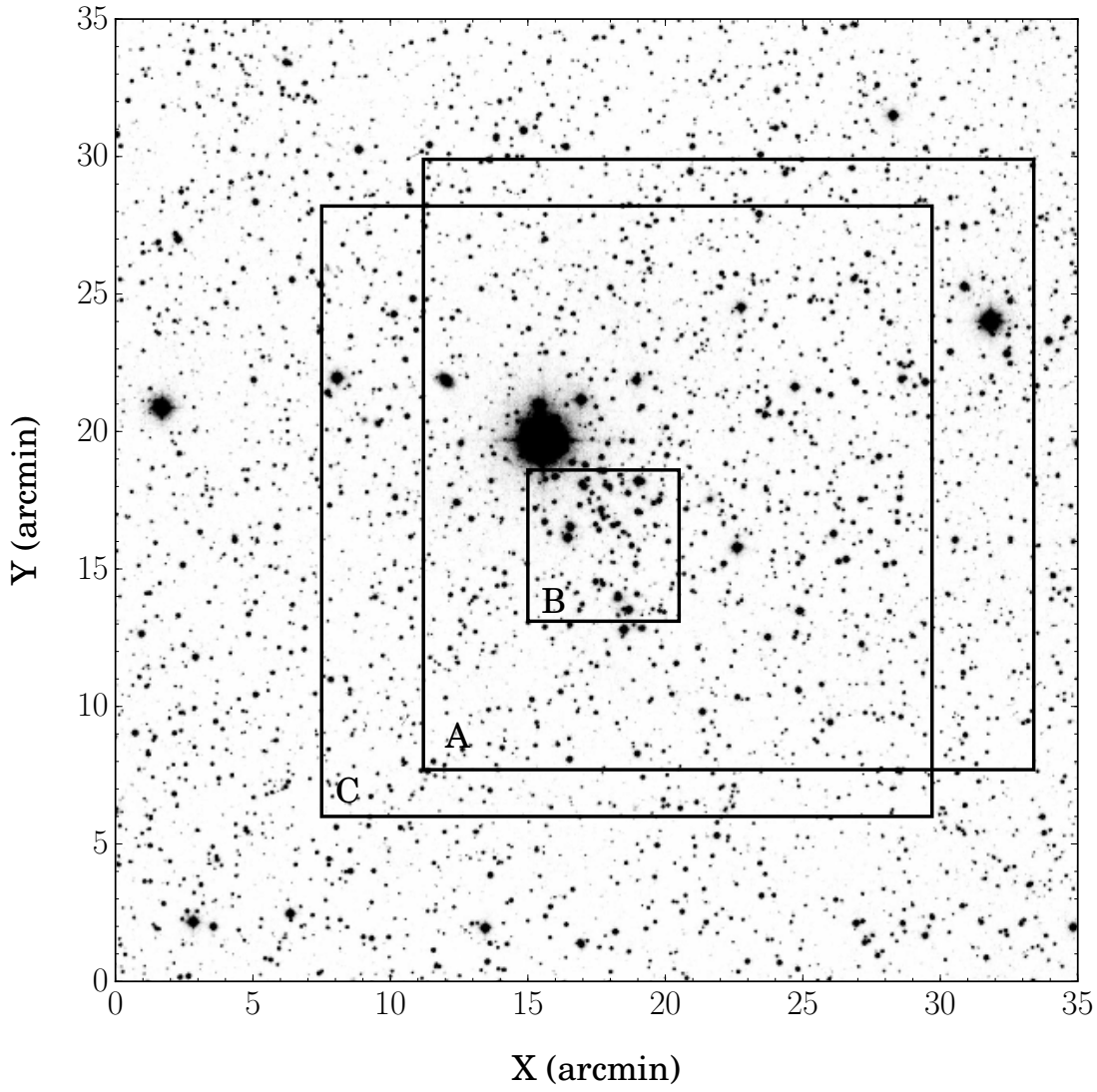

Figure 3.7: A Digitized Sky Survey (DSS) image of NGC 2126 ($35' \times 35'$, north is up, east is to the left). The three red boxes show the fields covered by our observations. The A field was observed with 1-m telescope (LOAO) in 2004, the smallest field named B was observed with 2.4-m telescope (TNO) in 2013, and the C field was observed with 0.5-m telescope (TNO) in 2015. See further details in Table 3.8.

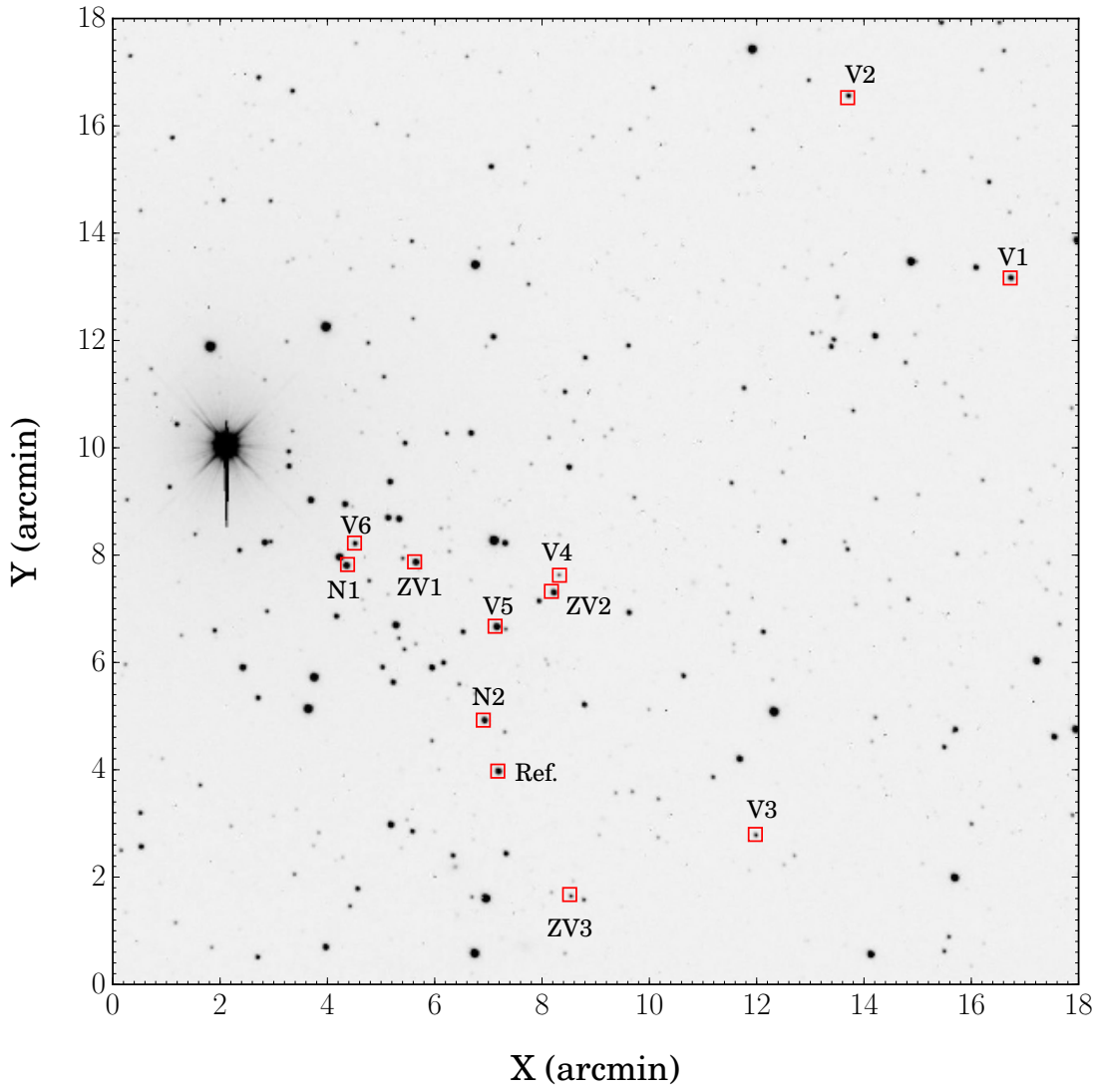

Figure 3.8: Finding chart for the variable stars in the field of NGC 2126 ($18' \times 18'$, north is up, east is to the left). The red open squares indicate 11 periodic variables identified in this study.

Table 3.7: The characteristics of the various telescopes, CCD cameras and size of field of view (FOV).

Obs.	Location	Telescope diameter (m)	Detector	FOV (arcmin^2)
LOAO	Arizona, USA	1	2k×2k CCD camera	22.2×22.2
TNO	Chiang Mai, Thailand	2.4	2k×2k Apogee U4200 CCD camera	5.5 × 5.5
TNO	Chiang Mai, Thailand	0.5	3056×3056 pixel Apogee Altra U9000 CCD camera	22.2×22.2
BHO	Brussels, Belgium	0.4	ST10XME CCD camera	17.2×25.5

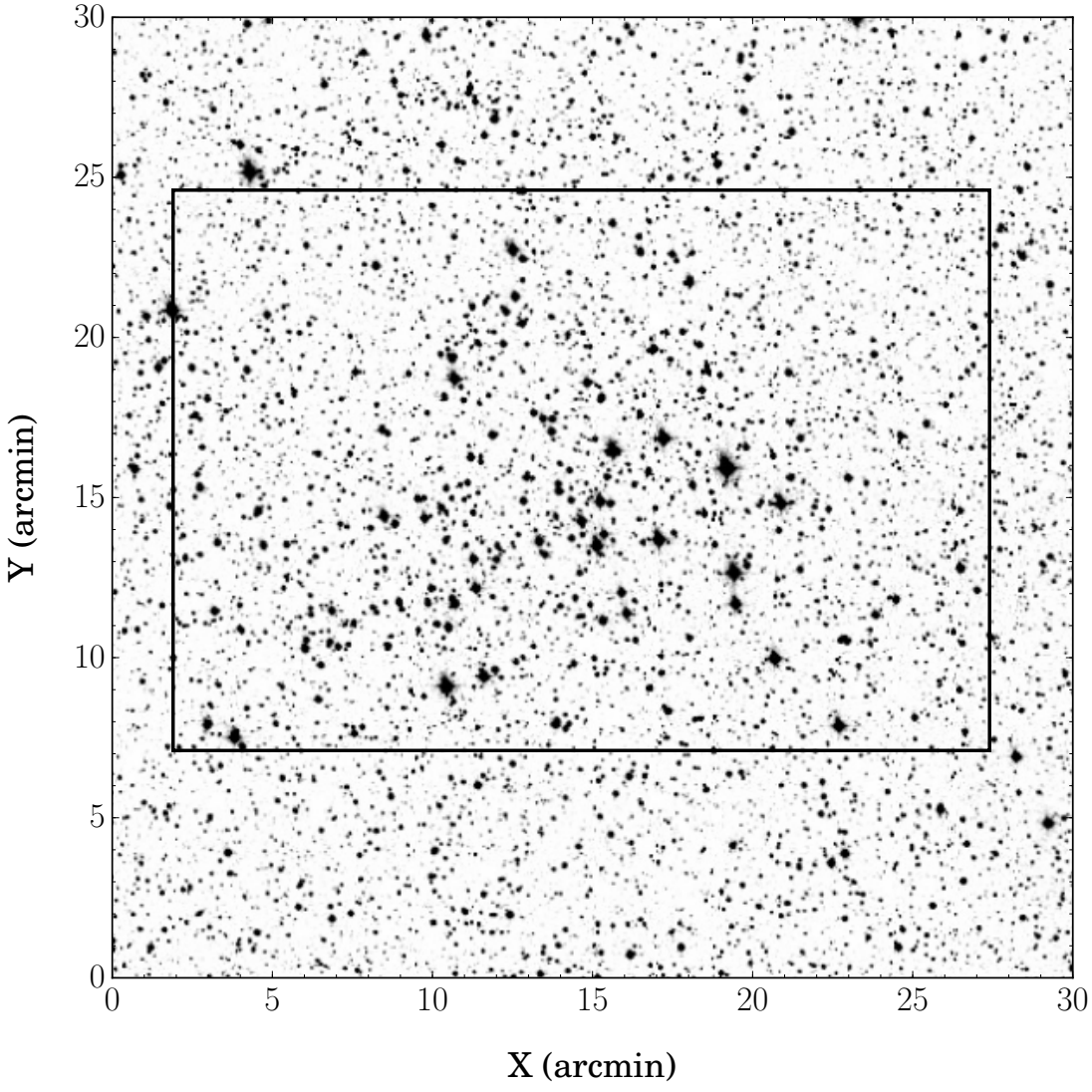

Figure 3.9: A Digitized Sky Survey (DSS) image of NGC 1528 ($30' \times 30'$, north is up, east is to the left). The black box shows the field covered by our observations. See further details in Table 3.9.

Table 3.8: The journal of observations of NGC 2126

Date (yyyy month dd)	Start time (HJD+2450000)	Length (Days)	No. of frames (filter V)
2004 March 24	3088.624144	0.178	50
2004 March 25	3089.617662	0.137	37
2004 March 26	3090.606447	0.192	86
2004 March 27	3091.608657	0.187	75
2004 March 28	3092.619317	0.173	68
2004 March 29	3093.611227	0.175	70
2004 March 30	3094.611308	0.174	72
2004 March 31	3095.622928	0.101	57
Total			515
2013 January 12	6305.123449	0.054	9
2013 January 13	6306.212188	0.195	23
2013 January 14	6307.135486	0.222	15
2013 February 5	6329.178681	0.147	44
2013 February 6	6330.084792	0.180	85
2013 February 7	6331.060556	0.225	112
2013 February 8	6332.042593	0.272	92
2013 February 9	6333.082940	0.208	76
Total			456
2015 March 16	7098.056933	0.123	84
2015 March 17	7099.020683	0.158	119
2015 March 18	7100.067743	0.108	89
2015 March 19	7101.008542	0.052	45
2015 March 20	7102.026655	0.040	34
2015 March 21	7103.023032	0.048	40
Total			411

Table 3.9: The journal of observations of NGC 1528

Date (yyyy month dd)	Start time (HJD+2450000)	Length (Days)	No. of frames (filter V)
2003 October 15	2928.4625580	0.165	96
2003 October 28	2941.3576160	0.108	58
2003 November 5	2949.2770950	0.190	100
2003 November 6	2950.3858100	0.188	107
2003 November 7	2951.2350690	0.342	116
2003 November 11	2955.2858450	0.182	63
2003 December 8	2982.4871880	0.164	202
Total			742
2006 September 21	4000.4152083	0.092	40
2007 February 3	4135.3197627	0.209	110
2007 February 21	4152.6571644	0.055	12
2007 February 22	4153.5828472	0.124	39
2007 February 27	4158.6102430	0.085	75
2007 March 5	4164.5749653	0.133	61
2007 March 8	4167.5725000	0.118	90
2007 March 9	4169.3260301	0.124	42
2007 March 11	4171.2875463	0.196	63
2007 March 12	4172.2955787	0.227	70
2007 March 25	4185.3304051	0.116	41
2007 March 26	4186.3130671	0.153	52
2007 March 27	4187.3020833	0.177	47
Total			742

Table 3.10: Coordinates from the catalogue of reference and check stars

Cluster	Name	UCAC4 Catalogue	RA(J2000)	Dec.(J2000)
NGC 2126	Reference star	700-043189	06:02:26.332	+49:50:02.35
	Check star 1	700-043225	06:02:34.704	+49:51:57.93
	Check star 2	700-043227	06:02:34.941	+49:51:12.88
NGC 1528	Reference star	706-029606	04:14:46.732	+51:08:04.83
	Check star 1	706-029686	04:15:16.155	+51:09:21.74
	Check star 2	707-030112	04:15:12.202	+51:17:35.36

3.3 Data Reductions

Time-series photometry was perform to search for variable stars in the clusters. A total of 1,382 time-series CCD frames of NGC 2126 was obtained with the V filter. Exposure times for all three observing runs were adjusted in a range from 100 to 300 s depending on sky conditions, seeing, and transparency. During the observations, the telescope's position was carefully controlled by fixing a star at the same position in the CCD frames to minimize position-dependent external errors (Frandsen et al., 1989). The CCD frame processing including subtraction bias frames, correction of flat fielding and trimming was performed using the standard routines of CCDRED in the IRAF package (Stetson, 1987). For flat field correction, sky flat images were taken in the evening and morning twilight. Then, we obtained the instrumental magnitudes using IRAF/DAOPHOT package and measured the differential magnitudes of all the stars in the field of view.

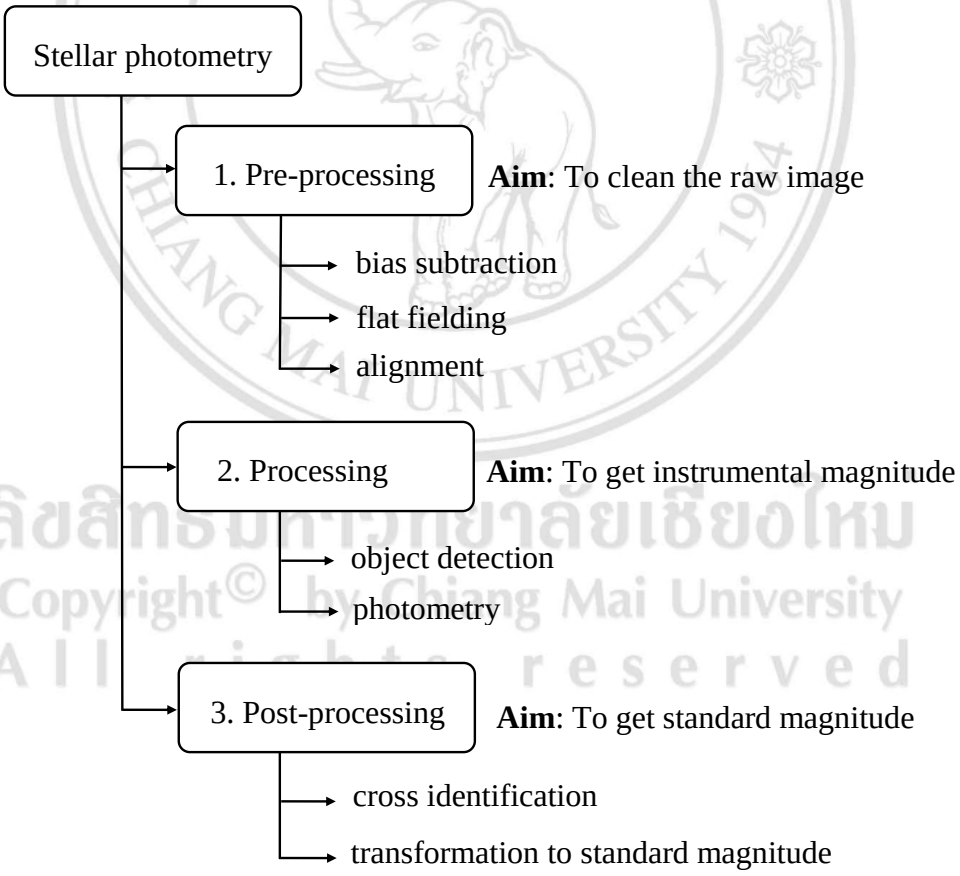

Figure 3.10: A flowchart of the stellar photometry using program IRAF

In the real observations, various artificial noises occur in the CCD images due to the

instrument itself. The distortion of light on the CCD images is affected by some defects or features of the instrument, therefore the light distribution in the image is not a reflection of the reality. It is necessary to use the process is called *basic image reduction* to remove or correct several features of the instrument before using images for scientific measurements. The images before reduction process are commonly called *raw images* while the images after reduction process are *science images*. In general, the basic data reduction of the CCD images consists of bias subtraction, flat fielding, dark subtraction, and in some cases shutter and non-linearity corrections. Each type of image and the standard ways of CCD frame processing are describes in the following sections.

3.3.1 CCD Image

A Charge Coupled Devices (CCD) is a rectangular area of sensors called *pixels*. The special characteristic of pixel is that can convert the incident light into charge (photons into electrons). Usually, the electrons produced in CCD is linearly proportional to a number of incident photon on each pixel. An exposure is the process of collected photon from the telescope fall onto the CCD. The CCD has a read-out circuit to read out signal pixel by pixel. Each pixel's charge in analog signal is transformed into a digital signal. This transformation is performed using an Analog-Digital Converter (ADC). In an electronic device, a digital number (DN) is shown as a series of number one and zero, which relate to two possible events. Finally, the ADC Converter provide a two dimensional array of numbers, each number is produced using the charge on each pixel. A two dimensional array of color distributions is displayed on the screen, a shade of color according to the number. For example, the highest number a completely white and a zero is perfect black. All numbers in between are some shades of grey, higher numbers resulting brighter ones, lower numbers resulting darker ones.

3.3.2 Bias Frames

Bias frames (zero frames) are zero exposure frames acquired keeping shutter of the CCD camera closed. The purpose of a bias frame is to allow the user to determine the underlying noise level within each data frame. While the CCD is collecting the light, the

electronics add some initial values to the CCD, the information will be biased in a way unique to each pixel. This bias for a given pixel exists even if no exposure time passes and no light is incident on the detector. The bias signal (or bias level) is uniform in every exposure and it is the uniform component that must be measured and subtracted from raw images. Bias frames should be acquired during the observations on regular intervals. An average bias image of more than ten single bias frames is recommended to use in this step, because a single bias frame will not sample the noise variations well in a statistical aspect (Howell, 2006). By collecting several of these frames, an average can be taken using IRAF task *zerocombine*, resulting *master bias* frame. A master bias frame provides a correction that can be applied to all other frames including flat and raw frames. In this procedure, no light is being measured, the filter is irrelevant and the same combined zero frame can be used for all filters used during the same night. For our observations, 11 bias frames were collected for each night. Then the bias frames are averaged to improve the signal-to-noise ratio (S/N). Finally, the bias frame is subtracted from all the raw images to remove the baseline count in each pixel.

3.3.3 Dark Frames

Dark frames are images taken with the shutter closed but for some time period, usually equal to that of the object frames. The importance of dark frames is that it can be used to measure the thermal noise (dark current) in a CCD. They provide information about *hot* or *bad pixels* that exist and also provide an estimate of the rate of cosmic ray strikes at the site. Observatory class CCD cameras are usually cooled with liquid Nitrogen to temperatures at which the dark current is essentially zero. Many of these systems therefore do not require the use of dark exposure CCD frames in the calibration process because the cooling systems are cooled to low enough temperatures. In addition, these less expensive models often have poor temperature stability allowing the dark current to wander a bit with time. The best way to produce the final dark calibration frame is average dark frames of more than ten images together. Note that the bias noise of the CCD also appears in dark frames, so separate bias frames substation are not needed.

3.3.4 Flat Fielding

Flat fields are taken to obtain a high S/N, uniformly illuminated calibration image. They can be taken either from the twilight sky, the nighttime sky, a dome screen, or a projector lamp. Flat field exposures are used to correct for pixel-to-pixel variations in the CCD response. In addition, they are also used to improve nonuniform illumination of the detector itself. Flat field calibration frames are required for each wavelength band, or different instrumental setup. For narrow-band system, flats are used to remove fringing, which occur in object frames. A good flat should remain constant to about 1%, with 2% or larger changes being indicators of a possible problem. At least five or more flat fields are need to average and produce the final flat used for image calibration (Howell, 2006). Bias subtracted flat frames are median combined to generate master flat using IRAF task *flatcombine*. This master flat is then normalized before correcting the science frames.

3.3.5 Object Frames

Object frames are the frames of the interested astronomical objects. They are of some exposure length from less than one second up to scale of hours depend on brightness of object, the science goal, and the other. Thermally generated electrons, read noise, contributions from the object and sky, and possibly contributions from cosmic rays are contained in the object frame. Non-uniformities in CCD image must be corrected, because each pixel does not respond similarly to the incident light. Standard CCD reductions can correct almost all of the noise in the object frame.

Table 3.11: Summary of the essential IRAF tasks which are needed for data reduction

IRAF Task	Description
zerocombine	Combine zero level images
flatcombine	Combine flat field images
ccdproc	Process CCD images by applying zero, flat, bad pixel corrections
ccdmask	Create a pixel mask from a CCD image
mkskyflat / *mkillumflat* / *mkillumcor* / *mkskycor*	Each of these tasks is meant to correct the illumination pattern in different ways

Table 3.12: Summary of some IRAF tasks for aperture photometry and calibration

IRAF Task	Description
daofind	Automatically detect stars and build a list of star coordinates.
phot	Do aperture photometry on a list of stars.
mkobsfile	Make a single observation file, matching up the corresponding observations in each of the filters.
fitparams	Given a set of observations and star catalog values, solve the transformation equations.
invertfit	Apply transformation equations to instrumental observations to obtain corrected extra-atmospheric star parameters.